Super Resolution, Time Reversal Focusing Using Path-Diverting Scatterers

Emily D. Golightly

A senior thesis submitted to the faculty of
Brigham Young University
in partial fulfillment of the requirements for the degree of

Bachelor of Science

Brian E. Anderson, Advisor

Department of Physics and Astronomy

Brigham Young University

April 2022

ABSTRACT

Super Resolution, Time Reversal Focusing Using Path-Diverting Scatterers

Emily D. Golightly
Department of Physics and Astronomy, BYU
Bachelor of Science

Time reversal is a process where a sound is recorded at a specific location, temporally reversed, and then played back to focus at the same location as the original recording. This thesis will focus on the use of near field scatterers in time reversal focusing to achieve super resolution. In particular, use of a one-dimensional pipe system with varying lengths of side branch pipes is shown to decrease the effective wave speed by forcing sound to travel a longer path from the source to the receiver as waves converge at the focal location. As the effective wave speed decreases, the spatial extent of the focusing decreases, creating super resolution. Previous work has achieved super resolution with resonators, and consequently, it has yet to be shown how scatterers can be used to obtain super resolution.

Keywords: time reversal, super resolution, path-diverting scatterers

ACKNOWLEDGMENTS

Funding was provided by the BYU College of Physical and Mathematical Sciences and Los Alamos National Laboratory, subcontract number 527136. I wish to thank Brian Anderson and Adam Kingsley for helping with experiment design, as well as for proofreading my code and my thesis. Rebekah Higgins also helped with conducting experiments and brainstorming solutions to problems we ran into along the way. I also wish to thank Jeremy Peterson and his students for helping create the pipe system used in these experiments.

I would also like to thank my family, especially my parents, for their continued support of my college education. Finally, I want to thank my fiancé, Samuel Dallon, for letting me talk through problems I encountered in experiments and coding, for offering suggestions when needed, and for helping me stay motivated to finish my college career strong.

Contents

List of Figures

List of Tables

Chapter 1

Introduction

Time reversal (TR) is a type of signal processing that can be used to focus waves to a specific point in space.[1-3] This is accomplished by recording an impulse response (IR) at a certain location, reversing it in the time domain, and broadcasting the reversed IR from either the original source or receiver locations. The first half of this process, known as the forward step, and the second half of the process, known as the backward step, can both be performed either experimentally or numerically. Here the source and receiver are kept in the same locations in the forward and backward steps and both steps are done experimentally. Because portions of the waves travel a similar path as they did initially, both directly through the medium and indirectly via reflections, broadcasting a reversed IR enables a focus to be created at the receiver location, which is a reconstruction of the originally broadcast signal.

TR has been used in focusing large amplitude sound, for communications, and to reconstruct sources in a variety of applications. It has been used to destroy kidney stones as a form of non-invasive surgery,[4,5] locate cracks in structures[3,6-8] find the epicenter of earthquakes and characterize their type of motion,[9] and locate the place a user taps on a touch screen device.[10] One current aim of TR research is in increasing the spatial resolution of the final focus, in order to better image the original source. The goal of such research is to achieve super resolution, which is resolution greater than the diffraction limit, commonly defined as a spatial peak in the far field

narrower than one half a wavelength of the signal, or $\lambda/2$,[11] at the full-width half maximum (FWHM) of a squared pressure distribution or of an energy or power distribution. However, for the spatial dependence of the pressure in a one-dimensional system, the FWHM diffraction limit is $\lambda/3$ because the aperture is restricted to one dimension. Although such resolution may initially appear to violate the established science behind the diffraction limit, a better explanation of this phenomenon may be that the assumptions of the diffraction limit are not met in cases where super resolution is achieved;[11] for example, focusing may occur in the near field of obstructions, rather than in an unobstructed far field. Here, super resolution means better resolution than can be achieved in a free-space medium, and thus the diffraction limit may not be technically broken.[11]

Many experiments that use TR to achieve super resolution involve placing objects in the near field of a source or receiver.[12-16] Resonators are the objects that have most often been used in TR super resolution research. Lerosy *et al.* conducted an experiment using electromagnetic waves and copper wires that achieved resolution of 1/16 the size of the diffraction limit (or up to $\lambda/32$).[12] While they referred to the copper wires as "resonant scatterers," the nature of electromagnetic waves inside of a wire suggests that these wires are more aptly considered resonators than scatterers. Other experiments have used the Helmholtz resonance of soda can resonators to achieve similar results with acoustic waves.[13] Other methods that have been used in achieving super resolution include using an acoustic sink,[14] using experimental or numerical absorbers,[15,16] and finally a technique that amplifies near field information.[17]

There are currently several explanations of how super resolution can be accomplished without breaking the diffraction limit. These explanations involve information contained only in the near field, and information lost in the transition from the near field to the far field. The near field is the area closest to a source, often within a fraction of a wavelength. In this area, waves interfere and

contort differently than they do once they reach the far field. In particular, the near field includes evanescent waves, which exponentially decay with distance from the source, and that are specific to the near-field conditions. When objects, such as resonators, are placed in the near field, it may disrupt the regular propagation of evanescent waves, enabling the information contained in these waves to be propagated into the far field, thus allowing the receiver to record a greater amount of data about the wave source than otherwise possible. With this additional information, the backwards step of TR can then reconstruct the source with better spatial resolution than it could otherwise.[12] It is also possible that measuring the near field information, and amplifying it, would enable its information to improve resolution in TR experiments.[17] The idea of an acoustic sink is to place an active source at the focal location that broadcasts opposite phase energy while energy is being focused in order to cancel out the far-field information, leaving only the near field information behind.[14] A technique known as sponge layer damping involves putting numerical absorbers around a focal location in order to suppress the converging far field information, making it easier to measure the near field information.[16] Finally, physical absorbers have been placed to surround a focal location in order to reduce the converging far-field information.[15]

Another possible explanation of the super resolution phenomenon is that objects close to the source and/or receiver force the wave to travel a longer path in order to cross the same effective distance.[18] As Maznev *et al*. described it, the objects form a medium for the wave to travel through that has a lower phase speed than the wave would have traveling outside of the medium.[19] Although the actual speed of the wave remains constant, the time required to travel the same effective distance is increased, thus reducing the effective wave speed. With a lower effective wave speed, the wavelength is also lowered, allowing the spatial extent of a focused signal to have a resolution smaller than the original diffraction limit.

Thus, while there are several studies that have shown super resolution can be achieved using resonators and other objects,[12-16] and several explanations have been offered as to how super resolution is possible in these experiments,[12,14-17] the use of a network of scatterers as a potential means to lower the effective wave speed to obtain super resolution has not yet been shown. Previous TR experiments using scatterers have investigated rotating scatterers between the forward and backward steps to show that this inhibits TR focusing,[20] but they did not explore the potential for achieving super resolution. Scatterers can be as simple as spheres or other geometrically creative objects and may provide a useful alternative to other approaches. The purpose of this thesis is to describe proof of concept experiments that show scatterers can be used to achieve super resolution. By forcing the waves to travel a longer path between measurement locations (traveling around a scatterer), the wave takes a longer time to traverse the distance it would have traveled had the scatterer not been present. The result is that the wave effectively travels at a lower speed, which leads to effectively shorter wavelengths.

First, the setup of the experiment will be described. Next, the results of the experiment will be given, as well as a description of a simulation model of the experiment and a comparison between these two. Possible explanations of the results will be discussed, and the thesis will conclude with the implications of this research and possible areas for future research.

Chapter 2

Experiment Setup

Experiments were conducted inside polyvinyl chloride (PVC) pipes of 1.905 cm (3/4 inch) inner diameter (Fig. 2.1). A pipe system was chosen in order to limit wave propagation to one dimension (the dimensions impose a plane wave cutoff frequency of about 10.5 kHz), and thus enable study of the simplest possible scattering network. PVC connectors were used to create a 9.14 m (30 feet) length pipe system out of three 3.05 m (10 feet) pipes. The overall length of the pipe system was chosen to allow for several closed-closed pipe resonances (along the pipe's length) to exist within the bandwidth used. The center 3.05 m pipe had 6.35 mm (1/4 inch) diameter holes drilled into it every 12.7 cm (5 inches), for a total of 23 holes. The holes were used as measurement locations, and were covered with sticky putty when a different location was being used, in order to prevent sound from leaking out of the pipe system. Measurements were made using a 6.35 mm (1/4 inch) GRAS (Holte, Denmark) 40BE free field microphone with a GRAS 12AX 4 channel power module. Two additional 3.05 m length pipes were connected on either end of the center pipe that did not have measurement location holes in them as part of the main trunk of the 9.14 m pipe length. The focal location (where the IRs are measured and the subsequent focusing occurs), the additional measurement locations, the extra main-trunk pipe lengths, the sources, and the amplifiers are indicated in Fig. 2.1.

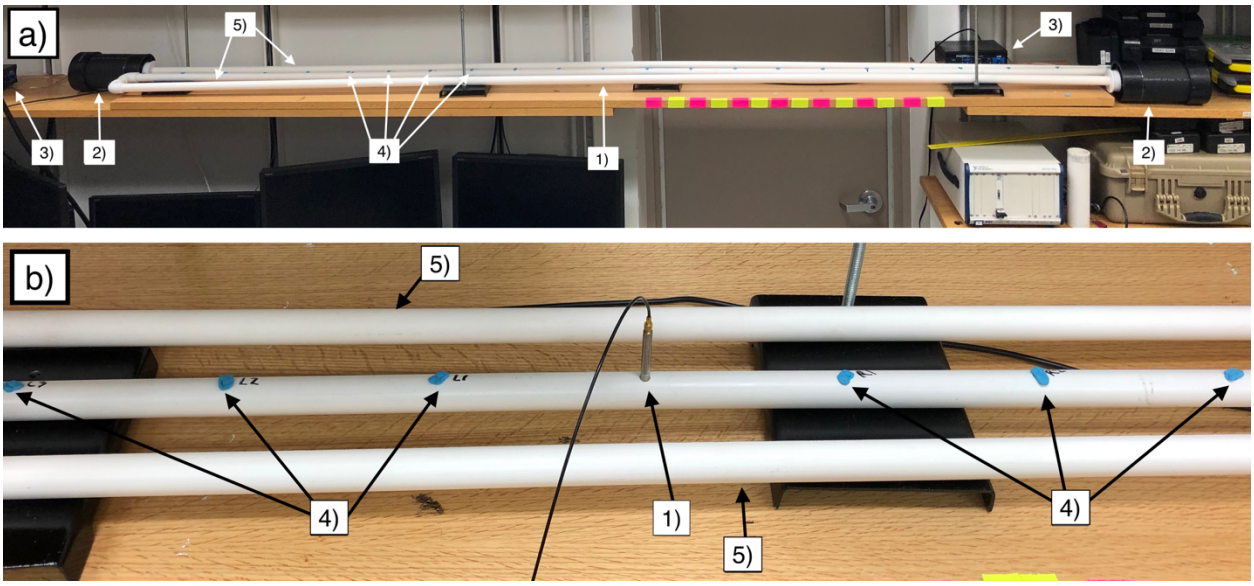

FIG. 2.1. (a) Photograph of the experimental setup for the control experiment, (b) Close-up photograph of the center portion of the control experiment setup. Items identified in the images: 1) Focal location, 2) Black-colored PVC pipes that house the sources, 3) Amplifiers, 4) Sampling at additional measurement locations, 5) Extra main-trunk pipe lengths.

At each end of the pipe system, a section of black-colored PVC pipe 10.2 cm (4 inch) inner diameter was attached and a Tang Band (Taipei, Taiwan) WS-881SJ loudspeaker driver was secured inside it (see Fig. 2.1, location 2). Two Pyle Pro (Brooklyn, New York) PCA3 stereo power amplifiers (Fig. 2.1, location 3) were used to provide power to the loudspeakers. Appropriate connectors and caps were placed on each end of the pipe system in order to ensure that the system had minimal sound leakage. All signals were generated and processed for TR using a custom in-house LabVIEW™ interface, coupled with two Spectrum (Großhansdorf, Germany) M2i.6022 signal generation cards and a Spectrum M2i.4931 digitizer card. All post-processing was handled in MATLAB™. The sampling frequency used throughout these measurements was 150 kHz.

In the forward step, the microphone was placed in the center receiver location (the previously determined focal location; see Fig. 2.1, locations 1) and all remaining holes were covered with sticky putty (Fig. 2.1, locations 4). A logarithmic chirp signal from 100 Hz to 500 Hz was played from a single loudspeaker, and a signal response was recorded by the microphone, as illustrated in Figs. 2.2(a) and 2.2(b), respectively. This chirp range was chosen due to its large wavelength, which enabled recording of the spatial extent of the time reversed focus at multiple locations within a single wavelength to compare to the diffraction limit. For any time signal recording discussed in these experiments, averaging was employed to reach each result through repetitions of the experiment.

The IR for the loudspeaker and microphone combination was calculated using a cross-correlation of the original chirp signal with the response recorded by the microphone when the loudspeaker plays the chirp signal.[21,22] This process was repeated for the second loudspeaker with the microphone in the same location, and the two IRs were then reversed in time and played simultaneously from their respective loudspeakers, creating a focus at the center receiver location (focal location), as in Figs. 2.2(c) and 2.2(d).

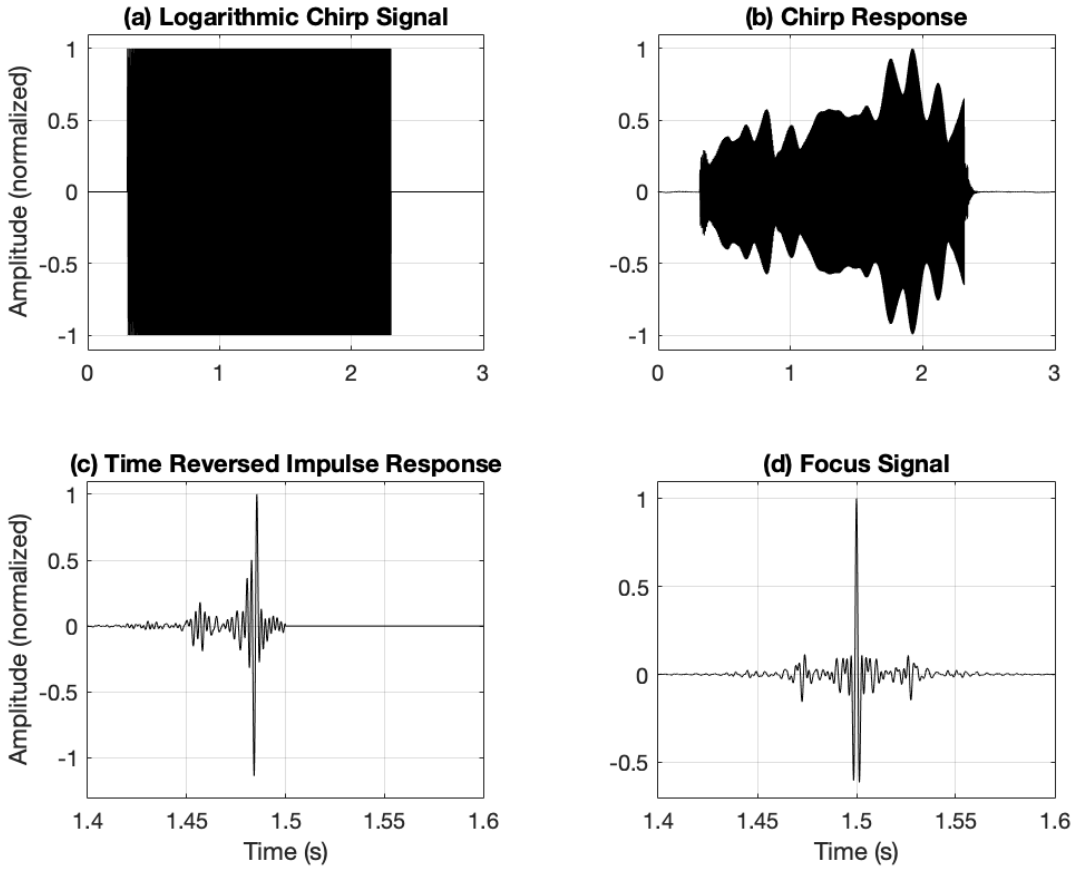

FIG. 2.2. Example signals for a time reversal experiment. (a) The chirp signal initially played from both loudspeakers. (b) An example chirp response recorded at the focal location. (c) A time reversed impulse response. (d) A focus signal recorded at the focal location, generated by both loudspeakers. Amplitudes in this figure were normalized.

After the focus was recorded at the focal location, the microphone was moved to the right one measurement location, and the two reversed IRs were played again, allowing measurement of the same focal event at a different point in space. This process was repeated for the remaining 21 measurement locations, and graphs of the spatial extent of the focus at the focus time were made in post-processing.

Once this control experiment was completed, the center 3.05 m pipe was removed from the pipe system and replaced with a pipe of the same length that included path diverting PVC pipes of 1.27 cm (1/2 inch) inner diameter, as shown in Fig. 2.3. The smaller diameter in the path-diverting pipes was used to increase the amount of scattering within the pipe system. These pipes left the plane of the original pipe system and came back within a 12.7 cm space, and were placed between the middle eleven receiver locations, for a total of ten path diversions (Fig. 2.3, locations 6). The pipe with the path diversions had holes drilled in the same receiver locations as the control pipe, and the same experiment was repeated with the new pipe system. A total of four different lengths of path diversions were used: 5.08 cm, 10.16 cm, 15.24 cm, and 30.48 cm pipes. Each path diversion pipe length mentioned actually added double its length between each measurement location; for example, the 5.08 cm pipes increased the total distance traveled within the pipe system between each receiver location from 12.7 cm to 22.86 cm.

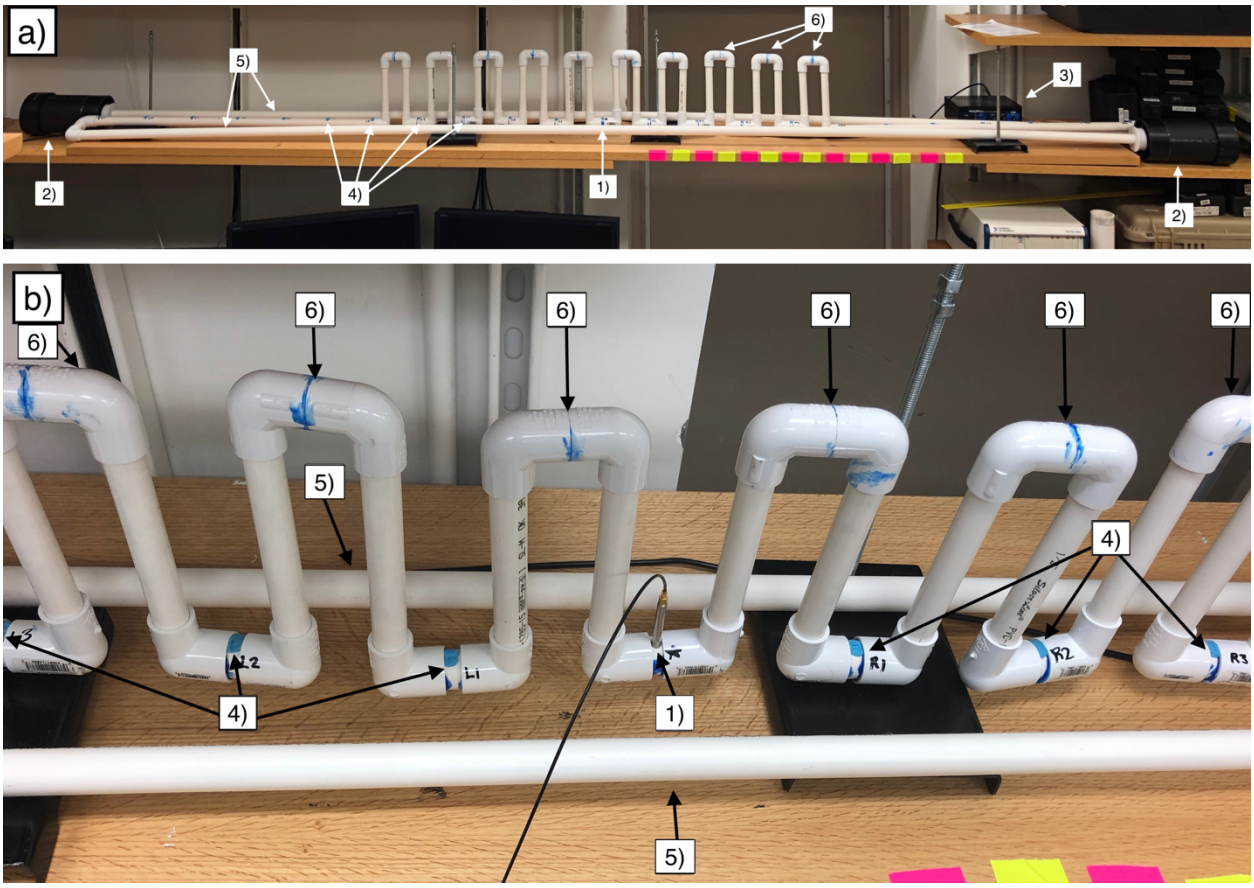

FIG. 2.3. (a) Photograph of the experimental setup including path-diverting scatterers, (b) Close-up photograph of the center portion of the experimental setup using path-diverting scatterers. Items identified in the images: 1) Focal location, 2) Black-colored PVC pipes that house the sources, 3) Amplifiers, 4) Sampling at additional measurement locations, 5) Extra main-trunk pipe lengths, 6) Sampling at path diversions added after control experiments were completed. This image shows the pipe system with 15.24 centimeter path diversions.

Chapter 3

Results

Super resolution was achieved in each of the spatial foci measured that used path-diverting scatterers. Table 3.1 lists the FWHM of each length of path diversions with respect to λ and in comparison to the diffraction limit ($\lambda/3$ as explained previously). As expected, the length of the path-diverting scatterers affected the FWHM, with longer path-diverting scatterers leading to improved resolution. In the control case (no path-diverting scatterers), resolution is seen to be slightly smaller than the diffraction limit; this is likely due to the relatively large distance between measurement points, which could mean that the focus peak is more rounded than the data indicates, which, when accounted for, yields diffraction-limited results.

TABLE 3.1. Length of path-diverting scatterers compared to the full-width at half maximum (FWHM) for the spatial extent of the focusing, shown with respect to smallest wavelength as well as with respect to the diffraction limit.

Length of Path-Diverting Scatterers (cm)	FWHM with Respect to Wavelength (λ)	FWHM with Respect to Diffraction Limit
0	λ/3.3	1.1 × better
5.08	λ/8.6	2.9 × better
10.16	λ/11	3.6 × better
15.24	λ/15	5.1 × better
30.48	λ/23	7.6 × better

Figure 3.1 shows the full spatial measurements of the control experiment and the experiment with 30.48 cm path diversions, which are the two most extreme cases in this study. The graph of the 30.48 cm path-diverting scatterers clearly has three peaks within the peak of the control measurement, which is unlikely to happen by accident, therefore indicating that the results show resolution well under the diffraction limit. Note that the spatial resolution of measurement locations isn't high enough to resolve the central peak's width with path-diverting scatterers in place.

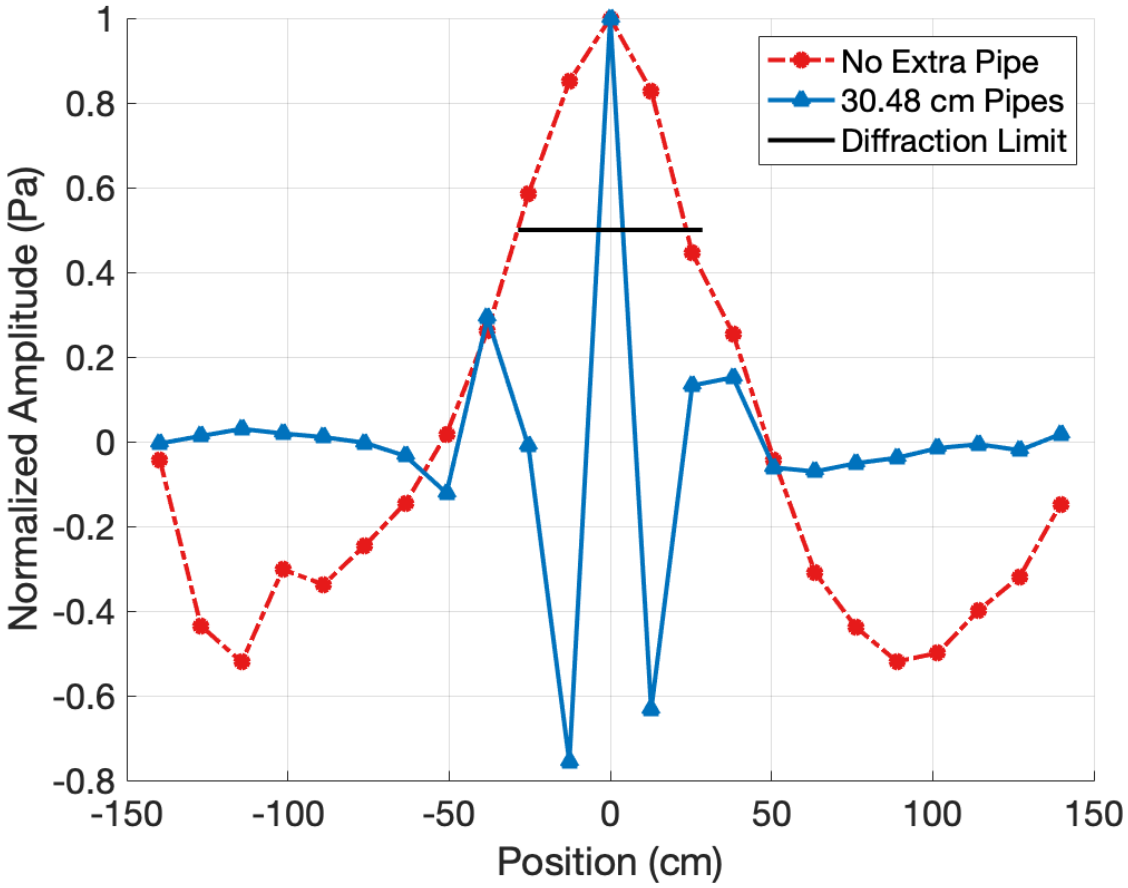

FIG. 3.1. Spatial plots of the pressure during time reversal focusing along the center pipe of the system, for the control experiment and the 30.48 cm path diversion experiment. The diffraction limit (λ/3) is shown with a black-colored solid line of length λ/3 as to give a reference. The control experiment is diffraction limited and is 1/7.6 the diffraction limit (λ/23) with the 30.48 cm path-diverting scatterers.

In order to explain the improved resolution due to the added path-diverting scatterer lengths, spectral information from the backward TR step was used to simulate the backward step. The path-diverting scatterers add length between the spatial measurement locations and this effectively spreads out the measurement locations further from each other with path-diverting scatterers

present. This simulation was done by taking a Fourier transform of the data taken at the measurement location two locations to the right of the focal location, in order to find the spectral amplitudes present in the data. This location was chosen to as being representative of the spectrum used in the experiments. These spectral amplitudes, A_f, were then used to create a simulated focus spatial distribution, $y_{simulated}$, based on a superposition of cosine waves as shown in Eq (3.1).

$$y_{simulated}(x_{trunk}) = \sum_f A_f \cos\left(\frac{2\pi f}{c}(x_{trunk} + N * L)\right), \tag{3.1}$$

where f is frequency, x_{trunk} is the horizontal position along the main trunk relative to the focus position, c is the speed of sound, and $N * L$ is the total length travelled through all intervening diversions, calculated by multiplying the length of an individual diversion by the number of diversions between the focus position and x_{trunk}. The cosine wave simplifies the summation by making all frequencies constructively interfere at $x = 0$.

This simulated focus spatial distribution, $y_{simulated}$, was then plotted in comparison to the experimental focus spatial distribution, and the process was repeated for each length of path-diverting scatterers. Figure 3.2 shows the simulated focus in comparison to the experimental focus for the 30.48 cm path diversions.

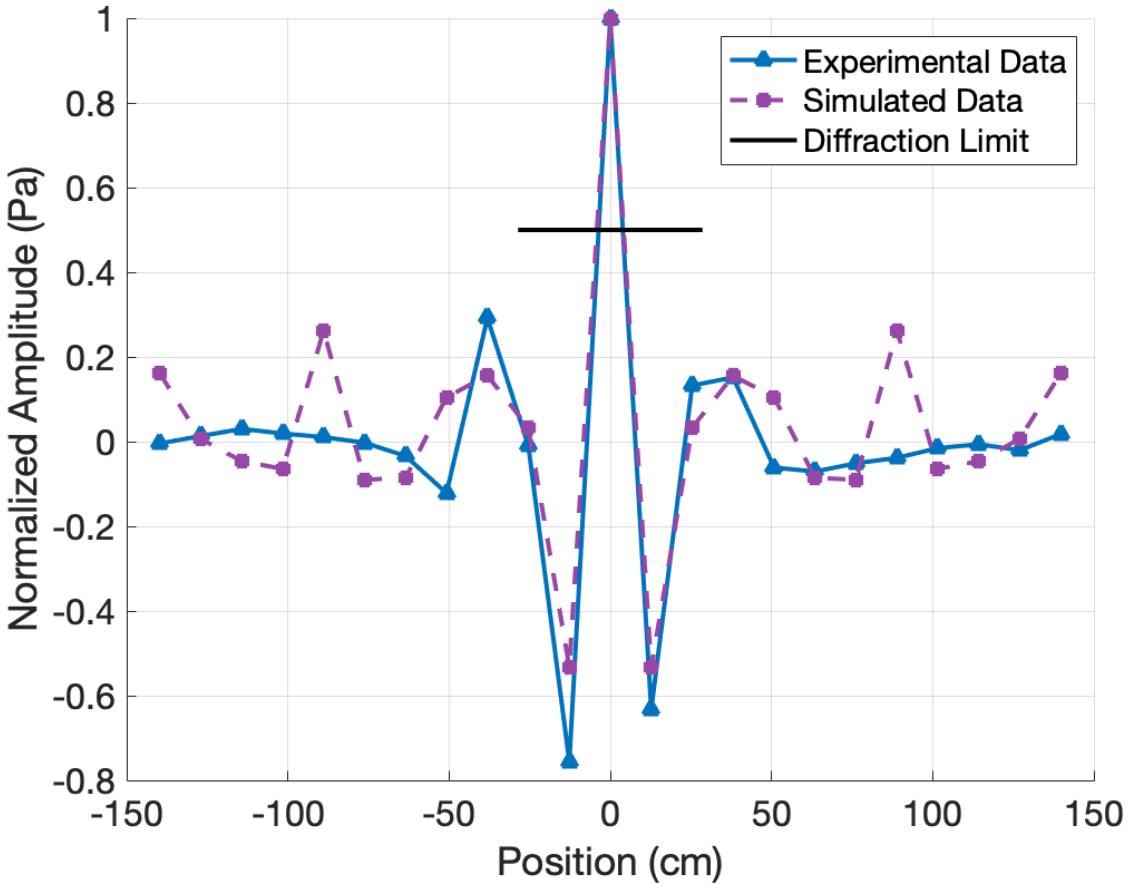

FIG. 3.2. Spatial focusing of 30.48 cm path-diverting scatterers, for the experimental and simulated data. The diffraction limit (λ/3) is shown with a black-colored solid line of length λ/3 as a reference.

Since the amplitudes of frequencies that are summed together were close to the focal location where the amplitudes of frequency components would be expected to be largest, the farther the measurement locations are from the focus, the less representative the frequency amplitudes would be for that location, leading to more variation between the simulated data and the experimental data. Significantly, the simulation is most accurate near the focus, where the frequency content is similar, including the size of the FWHM. This indicates that the simulation provides a reasonably

accurate estimation of the experimental results that can be obtained if one were considering adding in path-diverting scatterers of a selected size.

After the simulated data was created for each length of path-diverting scatterers, the FWHM was calculated for the experimental and simulated data corresponding to each length of path-diverting scatterers. This data is plotted in Fig. 3.3. As shown, all lengths of path-diverting scatterers included in the experiments and simulations provided super resolution, with the simulated data consistently having slightly worse resolution than the experimental data. As expected, as the path diversions are made to be longer, the effective wave speed is decreased and this leads to a smaller FWHM.

In the control experiment, the difference between the experimental FWHM and the simulated FWHM is significant. This could be caused, in part, by the large distance between measurement locations, which could lead to a peak that is more rounded than shown in the data collected. This would cause the experimental FWHM to increase slightly, putting it above the diffraction limit. Since the simulated data may already exhibit more rounding than the experimental data, such an error would have a lesser impact on the FWHM of the simulated data. In addition, this would have a more significant impact on a wider peak, as a smaller FWHM would have a less significant difference between a rounded peak and a sharp peak.

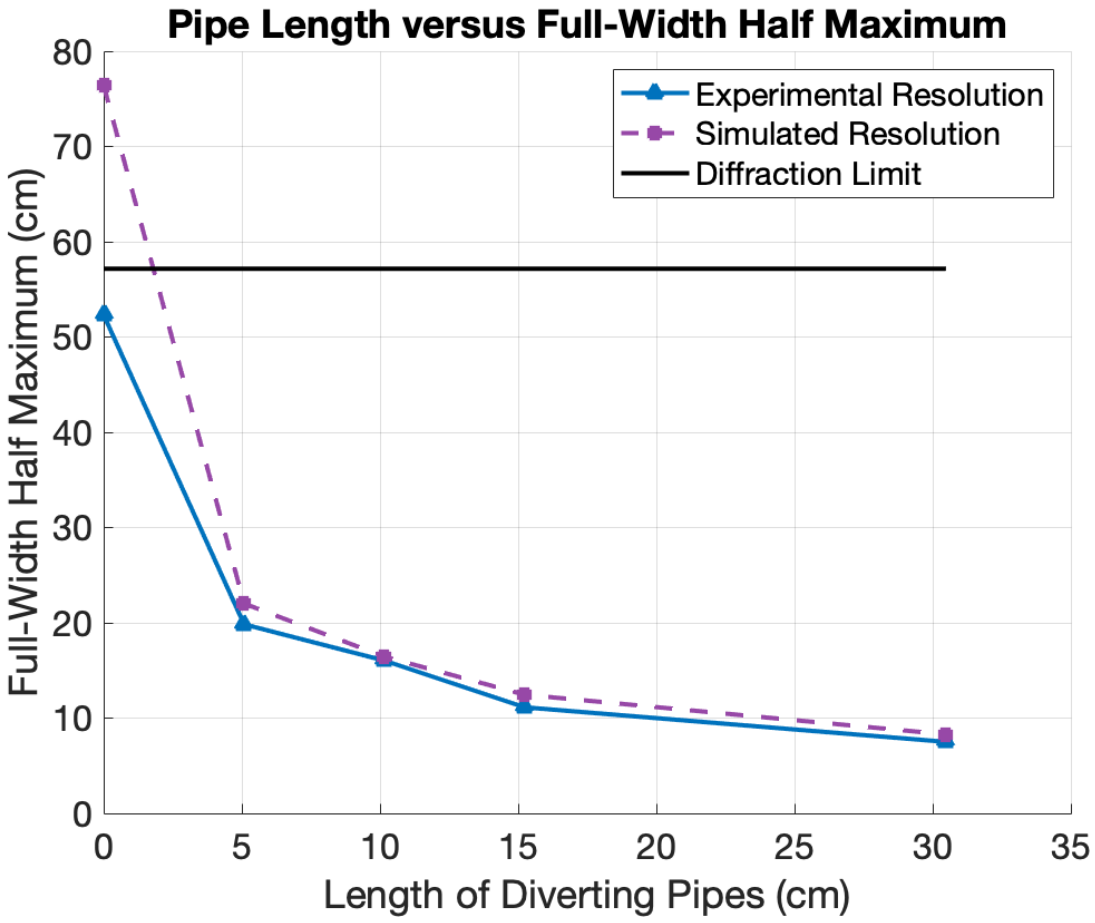

FIG. 3.3. Comparison of the length of diverting pipes with the full-width at half maximum measurements for both experiment and simulation data.

Chapter 4

Conclusion

This research has shown that super resolution can be achieved using time reversal (TR) with path-diverting scatterers. As waves are forced to divert around scatterers, the effective wave speed in the medium decreases, resulting in smaller effective wavelengths, and therefore improved resolution. The width of the peak depends on the length of the path diversions, with a longer path diversion corresponding to a narrower focus peak. This experiment showed super resolution up to 1/7.6 the diffraction limit (λ/23 resolution), using 61 cm path diversions placed between each measurement location that were spaced 12.7 cm apart. Super resolution was also observed even with 10.1 cm path diversions, although this resolution was only 1/2.9 the diffraction limit (λ/8.6 resolution). Simulations were shown to agree with these data, which proves that the path diversions simply increase the distance between measurement locations and thereby decreases the effective wave speed. Simulated TR yielded similar, although slightly more conservative, results.

It is important to note that, although the results of this experiment show improved spatial focusing resolution, the one-dimensional nature of the experiment limits the direct application of these results in two and three dimension TR experiments. Further research is needed to explore these effects in multiple dimensions. This thesis has, however, shown that the concepts behind the use of scatterers to achieve super resolution via slowing down the effective wave speed as waves divert around scatterers are sound and may be a viable alternative to using resonators and other

objects in the near field. If path-diverting scatterers are not possible or desirable to use, scattering objects of larger size should yield the same effects.

The results of this research suggest that it may be possible for scatterers to provide super resolution in TR. Previous research focused on the use of resonators or absorbers to enable super resolution, but it has now been demonstrated that scatterers may be used. This would be beneficial to super resolution research and applications in providing another method with which super resolution can be achieved, which may be a better alternative to current options in some situations.

References

[1] M. Fink, "Time reversed acoustics," *Phys. Today*, **50**(3), 34-40 (1997).

[2] B. E. Anderson, M. Griffa, C. Larmat, T. J. Ulrich, and P. A. Johnson, "Time reversal," *Acoust. Today* **4**(1), 5-16 (2008).

[3] B. E. Anderson, M. C. Remillieux, P.-Y. Le Bas, and T. J. Ulrich, "Time reversal techniques," Chapter 14 in Nonlinear Acoustic Techniques for Nondestructive Evaluation, 1st Edition, Editor Tribikram Kundu, ISBN: 978-3-319-94476-0 (Springer and Acoustical Society of America), pp. 547-581 (2018).

[4] G. Montaldo, P Roux, A. Derode, C. Negreira, and M. Fink, "Ultrasound shock wave generator with one-bit time reversal in a dispersive medium, application to lithotripsy," *Appl. Phys. Lett.* **80**(5), 897-899 (2002).

[5] A. Sutin and H. Salloum, "Prospective medical applications of nonlinear time reversal acoustics," *Proc. Meet. Acoust.* **34**(1), 020003 (2018).

[6] B. E. Anderson, M. Griffa, T. J. Ulrich, P.-Y. Le Bas, R. A. Guyer, and P. A. Johnson, "Crack localization and characterization in solid media using time reversal techniques," *Am. Rock Mech. Assoc.*, #10-154 (2010).

[7] B. E. Anderson, L. Pieczonka, M. C. Remillieux, T. J. Ulrich, and P.-Y. Le Bas, "Stress corrosion crack depth investigation using the time reversed elastic nonlinearity diagnostic," *J. Acoust. Soc. Am.*, **141**(1), EL76-EL81 (2017).

[8] S. M. Young, B. E. Anderson, S. M. Hogg, P.-Y. Le Bas, and M. C. Remillieux "Nonlinearity from stress corrosion cracking as a function of chloride exposure time using the time reversed elastic nonlinearity diagnostic," *J. Acoust. Soc. Am.*, **145**(1), 382-391 (2019).

[9] C. S. Larmat, R. A. Guyer, and P. A. Johnson, "Time-reversal methods in geophysics," *Phys. Today* **63**(8), 31–35, (2010).

[10] R. K. Ing, N. Quieffin, "In solid localization of finger impacts using acoustic time-reversal process," *Appl. Phys. Lett*. **87**(20), 204104 (2005).

[11] A. A. Maznev and O. B. Wright, "Upholding the diffraction limit in the focusing of light and sound," *Wave Mot.* **68**, 182–189 (2017).

[12] G. Lerosey, J. de Rosny, A. Tourin, and M. Fink, "Focusing beyond the diffraction limit with far-field time reversal," *Science* **315**(5815), 1120–1122 (2007).

[13] F. Lemoult, M. Fink, G. Lerosey, "Acoustic resonators for far-field control of sound on a subwavelength scale," *Phys. Rev. Lett.* **107**(6), 064301 (2011).

[14] J. de Rosny and M. Fink, "Overcoming the Diffraction Limit in Wave Physics Using a Time-Reversal Mirror and a Novel Acoustic Sink," *Phys. Rev. Lett.* **89**(12), 219901 (2002).

[15] G. Ma, X. Fan, F. Ma, J. de Rosny, P. Sheng, and M. Fink, "Towards anti-causal Green's function for three-dimensional sub-diffraction focusing," *Nat. Phys.* **14**(6), 608–612 (2018).

[16] A. Mimani, "A point-like enhanced resolution of experimental Aeolian tone using an iterative point-time-reversal-sponge-layer damping technique," *Mech. Sys. Sig. Proc.* **151**, 107411 (2021).

[17] S. G. Conti, P. Roux, and W. A. Kuperman, "Near-field time-reversal amplification," *J. Acoust. Soc. Am.* **121**(6), 3602 (2007).

[18] A. Azbaid El Ouahabi, L. Chisari, and G. Memoli. "Analytical and experimental investigation of the transmission/reflection coefficient from labyrinthine metamaterials," *Proc. Meet. Acoust.*, **42**, 065003 (2020).

[19] A. A. Maznev, G. Gu, S. Y. Sun, J. Xu, Y. Shen, N. Fang, and S. Y. Zhang. "Extraordinary focusing of sound above a soda can array without time reversal," *New J. Phys.*, **17**(4), 042001 (2015).

[20] V. S. Gomez, I. Spiousas, and M. C. Eguia. "Time reversal focusing in the audible range using a tunable sonic crystal," *J. Acoust. Soc. Am.*, **149**(6), 4024-4035 (2021).

[21] B. E. Anderson, M. Clemens, and M. L. Willardson, "The effect of transducer directivity on properties of time reversal focusing," *J. Acoust. Soc. Am.*, **139**(4), 2083–2083 (2016).

[22] B. Van Damme, K. Van Den Abeele, Y. Li, and O. Bou Matar, "Time reversed acoustics techniques for elastic imaging in reverberant and nonreverberant media: An experimental study of the chaotic cavity transducer concept," *J. Appl. Phys.* **109**(10), 104910 (2011).